J. Mater. Environ. Sci. 7 (8) (2016) 2718-2730
ISSN : 2805-2508
CODEN: JMESCN

Synthesis and inhibition study of carbon steel corrosion in hydrochloric acid of a new surfactant derived from 2-mercaptobenzimidazole

L. El Ouasif[1], I. Merimi[2], H. Zarrok[2], M. El ghoul[1], R. Achour[1], M. Guenbour[3], H. Oudda[2], F. El-Hajjaji[4,*], B. Hammouti[5]

[1] *Laboratoire de Chimie Organique Hétérocyclique, Université Mohammed V, Faculté des Sciences, Rabat, Morocco*
[2] *Laboratory of Separation Processes, Université Ibn Tofail, Faculté des Sciences, Kenitra, Morocco*
[3] *Laboratory of Nanotechnology, Materials & the Environment University Mohammed V, Faculté des Sciences, Rabat, Morocco*
[4] *Laboratoire d'Ingénierie d'Electrochimie, Modélisation et d'Environnement (LIEME), Faculté des sciences/Université Sidi Mohammed Ben Abdellah, Fès, Maroc*
[5]*Laboratoire de chimie analytique appliquée, matériaux et environnement (LC2AME), COSTE, Faculté des Sciences, Oujda, Morocco.*

Received 2 May 2016, Revised 18 June 2016, Accepted 21 June 2016
[*]*Corresponding Author. E-mail: el.hajjajifadoua25@gmail.com ;*

Abstract
In this paper, we report a new surfactant (1-tetradecyl-2-(tetradecylthio)-1H-benzimidazole (T1)) derived from 2-mercaptobenzimidazole acting as a carbon steel corrosion inhibitor was synthesized. The molecule structure was confirmed by means of chemical ionization of mass spectrometry, ^{1}H and ^{13}C nuclear magnetic resonance. EIS and potentiodynamic polarization measurements as well as scanning electron microscopy were used to evaluate the corrosion inhibition of T1 for C-steel in HCl. The results of EIS indicate the increase of transfer resistance with the increase of inhibitor concentration. Electrochemical measurements indicate that T1 is a mixed type inhibitor. It has been found that the studied compounds adsorb onto carbon steel according to the modified Langmuir adsorption isotherm and the kinetic/thermodynamic isotherm of El-Awady. The inhibition mechanism was explored by the potential of zero charge (Epzc) measurement at the solution/metal interface. Dynamic simulation indicates the possibility of gradual substitution of water molecules from the surface of iron surface.

Keywords: 2-mercaptobenzimidazole, hydrocarbon chains, carbon steel, corrosion inhibition, hydrochloric acid.

1. Introduction
Surfactants have been widely used as corrosion inhibitors for different metals in different corroding media. Their use is discussed for various metals such as C-steel [1-3] Cu [4,5] and Al [6,7]... The surfactants with double chain have specific properties outcome from the ambivalence of their chemical structure. They consist of a polar hydrophilic head and two hydrophobic tails that give them an ability to self-organize into a double sheet. Due to these particular properties of the surface, the double-chain surfactants have several applications both in the field of chemistry [8], in the biological and biomedical field [9].
Cationic, anionic and non-ionic surfactants [10-12] have been used as corrosion inhibitors for iron and steels in both HCl and H_2SO_4 solutions.

The choice of a surfactant as an inhibitor depends both on the metal and the composition of the corroding medium. Usually, the hydrophilic moiety of the surfactant adsorbs on the metal surface while the

hydrophobic moiety extend on the solution face. Two modes of adsorption on the metal surface are considered: Chemical adsorption takes place through charge transfer between certain delocalized π-electrons of the molecule and the empty d-orbital of the iron surface atom, and/or physical adsorption takes place through Van der Waals forces or electrostatic attraction [13-15]. The increase in the number of carbon atoms in the hydrophobic part has its impacts on the inhibition efficiency of the surfactant [16]. The inhibitory effect is generally explained by the intramolecular synergistic effect of various groups of the inhibitor. Our focus is to combine surfactant with a large studied molecule, benzimidazole known by their inhibiting action [17-21]. Over the years of active research, benzimidazole has evolved as an important heterocyclic system due to its presence in a wide range of bioactive compounds like antimicrobials, antivirals, antiparasites, anticancer, anti-inflammatory, antioxidants, proton pump inhibitors, antihypertensives, anticoagulants, immunomodulators, hormone modulators, CNS stimulants as well as depressants, lipid level modulators and antidiabetics [22-28]. Thus, this compound has more active sites, giving it great responsiveness, making it an excellent precursor for the synthesis of new compounds may present interesting surfactant properties.
The aim of the present study is to evaluate the corrosion inhibition efficiency of carbon steel in (1M) hydrochloric acid solution of 1-tetradecyl-2-(tetradecylthio)-1H-benzimidazole (T1) newly synthesized.

2. Experimental details

2.1. Synthesis of inhibitors

To a solution of 2 g (133.10^{-4} mol) of 2-mercaptobenzimidazole and 80 ml of N,N-dimethylformamide was added 3.67g (266.10^{-4} mol) of potassium carbonate, ($13.3.10^{-4}$ mol) of tetra-n-butylammonium bromide and 5.11g (399.10^{-4} mol) of 1-bromotetradecane.
The reaction mixture was stirred at room temperature for 24 hours. After filtration, the solvent was removed under reduced pressure. The residue is taken up in dichloromethane, filtered and the solvent was evaporated under reduced pressure (**Fig 1**).

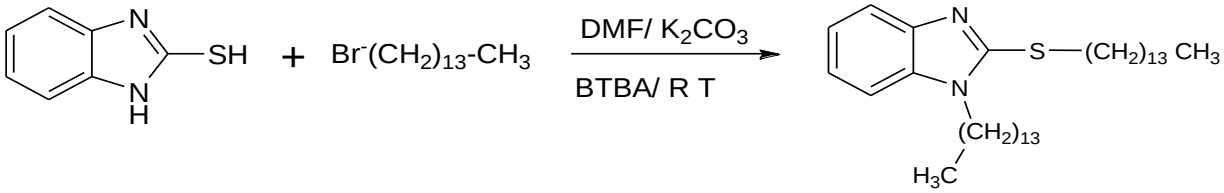

Fig 1 : Synthesis of 1-tetradecyl-2-(tetradecylthio)-1H-benzimidazole (T1)

Yield = 97%, NMR^{1}H ($CDCl_3$) (δ ppm): 0.86: (t, 6H, $–CH_3$); 1.23-1.81: (m, 48H, $–CH_2$); 3.51: (m, 2H, SCH_2); 4.09: (t, 2H, NCH_2); 7.23-7.79: (m, 4H, $CH_{benzene}$). NMR^{13}C ($CDCl_3$) (δ ppm): 14.1: (CH_3); 24.22-33.12: ($–CH_2$): 44.56 (SCH_2); 45.19: (NCH_2); 109.04-135.07: ($CH_{benzene}$); 151.95: (C=N). Mass spectrometry present a pic $[MH]^{\cdot +}$ at m/z= 543

2.2. Electrochemical experiments

A three electrode cell assembly containing carbon steel coupons of 1 cm² of surface, embedded in specimen holder as the working electrode (WE), a large area platinum mesh as counter electrode (CE) and a saturated calomel electrode as reference electrode (RE) were used. All electrochemical experiments were conducted at room temperature (308 ± 2 K) using 100 ml of electrolyte (1 M HCl) in stationary condition. Before each potentiodynamic polarization (Tafel) and electrochemical impedance spectroscopy (EIS) experiments the electrode was allowed to corrode freely and its open-circuit potential (OCP) was recorded as a function of time up to 30min. After this time a steady-state OCP, corresponding to the corrosion potential (E) of the working electrode, was obtained. The potentiodynamic Tafel measurements were started from cathodic to the anodic direction, between -800 mV and -200 mV with a scan rate of 1.0 mV. s^{-1}. The above procedures were repeated for each concentration of T1. Electrochemical impedance spectroscopy (EIS) measurements were carried out using ac signals of amplitude10 mV peak to peak in the frequency range of 100 kHz -10 mHz.

2.3. Simulation details

Molecular dynamics (MD) simulation was carried with the Metropolis Monte Carlo (MC) simulations methodology using the adsorption locator and Forcite code simplemented in the Material Studio 7.0 software commercialized by Accelrys Inc. USA [29]. The methodology and the procedure involved using the MC simulations can be found elsewhere [30-33]. The molecular dynamic calculation of the simulation of the interaction between the inhibitor molecule and the iron surface Fe (111) was carried out in a simulation box (35.17A° x 35.37A° x 40.26A°) with periodic boundary conditions to model a representative part of the interface devoid of any arbitrary boundary effects. The iron surface Fe(111) was first built and relaxed by minimizing its energy using molecular mechanics, then the surface area of iron surface Fe(111) was increased and its periodicity is changed by constructing a super cell (7*7), and then a vacuum slab with 30 Å thicknesses was built on the iron surface Fe (111) [34]. 30 molecules of water were added to simulate the effect of solvent since corrosion takes place in aqueous solution.

3. Results and Discussion

1. Electrochemical impedance spectroscopy (EIS)

Figure 2 shows Nyquist plots of C-steel immersed in molar hydrochloric acidic solution containing T1 at various concentrations at 308 K. Notice from this Figure that the Nyquist impedance semicircles increase with increasing content of the inhibitor. In other words, the diameter of the capacitive loop increases with increasing T1 concentration indicating increasing coverage of the metal surface. This implies that T1 adsorb on the metal surface to retard corrosion process.

The impedance diagram does not show perfect semicircle. This behavior can be attributed to the frequency dispersion [34-36] as a result of roughness and inhomogeneous of the electrode surface. Increase in the diameters of the semicircles with the concentration of the additive indicates that an increase of protective properties of the C-steel surface. Thus, the capacitive semicircle is correlated with the dielectric properties and the thickness of barrier adsorbed film [36]. Some impedance parameters such, as charge transfer R_t, and the double layer capacitance C_{dl} are derived from Nyquist plots and are given in Table 1 for C-steel in 1 M HCl solution in the presence and absence of T1. The decreased values of double layer capacitance, C_{dl}, may be due to the replacement of water molecules at the electrode interface by organic inhibitor molecules of lower dielectric constant through adsorption [37].

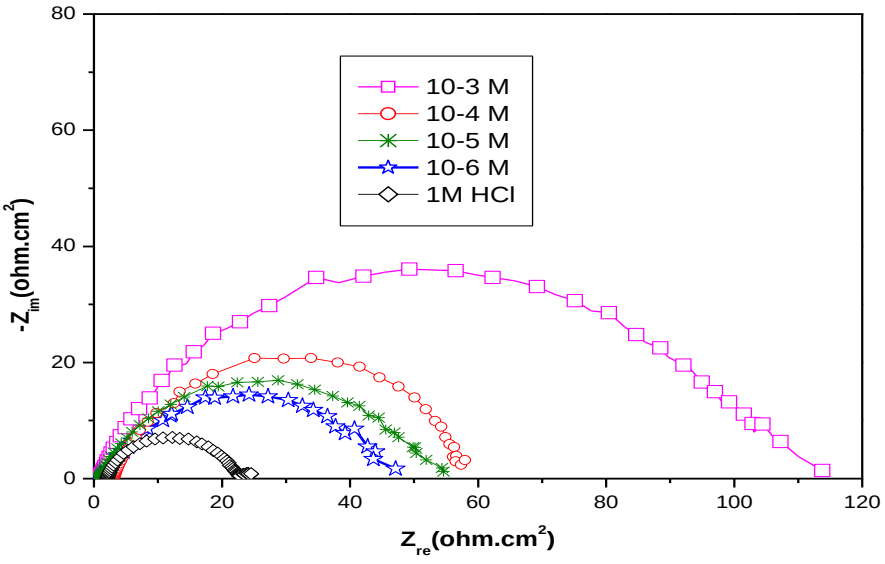

Fig. 2. Impedance plots of carbon steel in 1 M HCl with or without T1 at 308 K

ISSN : 2805-2508
CODEN: JMESCN

The charge-transfer resistance (R_t) values are calculated from the difference in impedance at lower and higher frequencies, as suggested. The inhibition efficiency got from the charge-transfer resistance is calculated by the following equation:

$$E\% = \frac{R'_t - R_t}{R'_t} \times 100$$

The R_t and R_t' are the charge-transfer resistance values without and with inhibitor respectively. Obtained E% values are also presented in Table 2.

From the impedance data (Table 1), we conclude that the value of R_t increases with increase in concentration of T1 and this indicates an increase in the corrosion inhibition efficiency. In fact, the presence of T1 enhances the value of R_t in acidic solution. Values of double layer capacitance are also brought down to the maximum extent in the presence of inhibitor. The decrease in C_{dl} is due to the adsorption of this compound on the metal surface leading to the formation of film from acidic solution [38]

Table 1: Kinetic parameters derived from EIS plots of M-steel in 1 M HCl containing T1 at 308 K

Concentration (mol/l)	**R_t (Ω cm^2)**	**R_s (Ω cm^2)**	**E_{corr} vs SCE (mV)**	**C_{dl} (μF/cm^2)**	**E (%)**
HCl 1M	**23.26**	**2.02**	-464	**149.8**	**-**
10^{-3}	108	1.9	-460	59.3	78
10^{-4}	57.75	1.875	-445	92.1	60
10^{-5}	53.46	0.66	-448	120.3	57
10^{-6}	44.4	1.87	-443	135.0	47

2. Potentiodynamic polarization

The polarization measurements are also made to the partial action of inhibitor on separated anodic and cathodic branches. The results obtained from electrochemical experiments are shown in Fig. 3 and Table 2. Values of cathodic β_c Tafel slopes and corrosion current density I_{corr} were calculated from the intersection of the anodic and cathodic Tafel lines of the polarization curves.

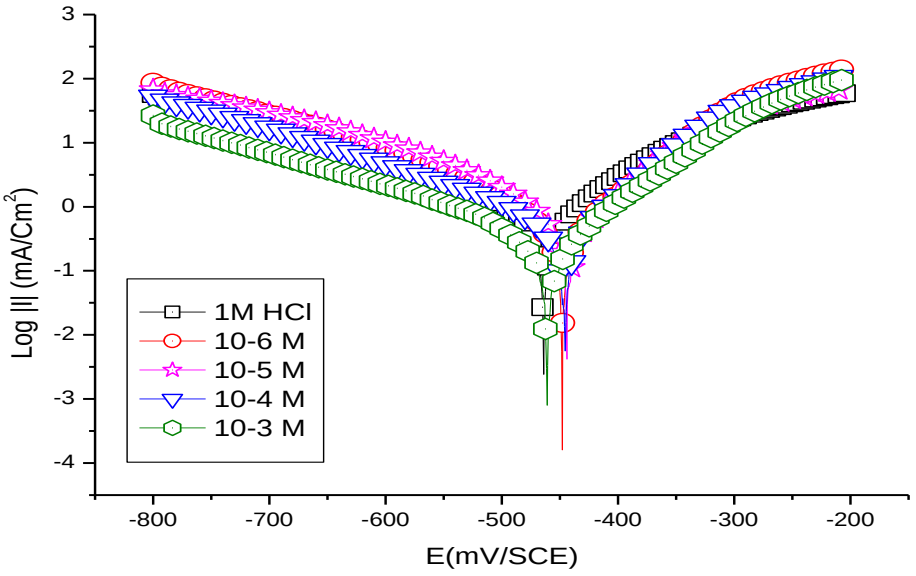

Fig. 3. Tafel plots of carbon steel immersed in 1 M HCl with or without T1.

The anodic and cathodic Tafel lines were almost parallel upon increasing inhibitor concentrations. This suggests that the hydrogen reduction at the metal surface is activation controlled and the mechanism is not affected by the presence of inhibitor [39,40]. The corrosion potential is almost constant and the change in E value is around 40 mV. According to Cao [41], the inhibitor acts by simple blocking the C-steel surface. The anodic and cathodic current densities are decreased at the presence of inhibitor, indicating that the inhibitor as amixed-type inhibitor. The inhibition efficiency is calculated by the following expression:

$$E\% = \frac{i_{corr} - i_{corr/inh}}{i_{corr}} \times 100$$

where i_{corr} and $i_{corr/inh}$ are respectively, the corrosion current density of carbon steel with and without T1 in HCl solutions.

Table 2: Kinetic parameters derived from Tafel plots of M-steel immersed in 1 M HCl containing T1

Concentration (M)	E_{corr} (mV/SCE)	I_{corr} ($\mu A\ cm^{-2}$)	$-\beta_c$ (mV/dec)	E (%)
HCl 1M	-464	2102.7	220	-
10^{-3}	-460	374.2	188	82
10^{-4}	-445	649.3	177	69
10^{-5}	-448	1085.2	187	48
10^{-6}	-443	1108.3	158	47

Examination of Table 2 reveals the cathodic Tafel slope (β_c) show slight changes with the addition of T1, which suggests that the inhibiting action occurred by simple blocking of the available cathodic sites on the metal surface, which lead to a decrease in the exposed area necessary for hydrogen evolution. In addition, the inhibitory action increases with the increasing of inhibitor concentration. At the concentration of 10^{-3} M or more, T1 acts as a good hydrochloride acid inhibitor with inhibition efficiency about 82%.

3. Adsorption isotherm and adsorption parameters

Adsorption of the organic compound depends upon the charge and the nature of the metal surface, electronic characteristics of the metal surface on adsorption of solvent and other ionic species, temperature of the corrosion reaction and the electrochemical potential at the metal solution interface [42]. Adsorption of the T1 involves two types of the possible interaction with the metal surface. The first one is weak undirected interaction due to electrostatic attraction between inhibiting organic ions or dipoles and the electrically charged surface of the metal. This interaction is termed physical adsorption or physisorption. The second type of interaction occurs when there is interaction between the adsorbate and adsorbent. This type of interaction involves charge sharing or charge transfer from adsorbate to the atoms of the metal surface in order to form a coordinate type bond and the interaction is termed chemical adsorption or chemisorptions [43].

Adsorption isotherms are usually used to describe the adsorption process. The most frequently used isotherms include Langmuir, Temkin, Frumkin, Hill deBoer, Parsons, Flory-Huggins, Dhar- Flory-Huggins, Bockris-Swinkels and thermodynamic/kinetic model of El-Awady et.al. [44-46].The adsorption isotherm provides important clues regarding the nature of the metal-inhibitor interaction. Inhibitor molecules adsorb on the metal surface if the interaction between molecule and metal surface is higher than that of the water molecule and the metal surface [47]. In order to obtain the adsorption isotherm, the degree of surface coverage (θ) for various concentrations of the inhibitor was calculated using equation below and listed in the Table 3.

$$\theta = \frac{R'_t - R_t}{R'_t}$$

Langmuir isotherm was tested for its fit to the experimental data. Langmuir adsorption isotherm is given by following equation:

$$\frac{C_{inh}}{\theta} = \frac{1}{K_{ads}} + C_{inh}$$

where C_{inh} is the inhibitor concentration, and K_{ads} the adsorptive equilibrium constant, θ representing the degree of adsorption.

The plot of the (C_{inh} /θ) vs C_{inh} fitted the experimental data did not follow the Langmuir adsorption isotherm. By testing other adsorption isotherms, it is found that the experimental data fits the El-Awady adsorption isotherm for concentrations range studied. The characteristic of the isotherm is given by:

$$Ln\left(\frac{\theta}{1-\theta}\right) = LnK + yLnC_{inh}$$

where, C_{inh} is molar concentration of inhibitor in the bulk solution, θ is the degree of surface coverage, K is the equilibrium constant of adsorption process; $K_{ads} = K^{1/y}$ and y represent the number of inhibitor molecules occupying a given active site. Value of 1/y less than unity implies the formation of multilayer of the inhibitor on the metal surface, while the value of 1/y greater than unity means that a given inhibitor occupy more than one active site [48,49]. Curve fitting of the data to the thermodynamic/kinetic model (El-Awady et. al.) is shown in Figure 4. The plot gives straight lines which show that the experimental data fits the isotherm. The value of K_{ads} and 1/y calculated from the El-Awady et.al. isotherm model is listed in Table 3.

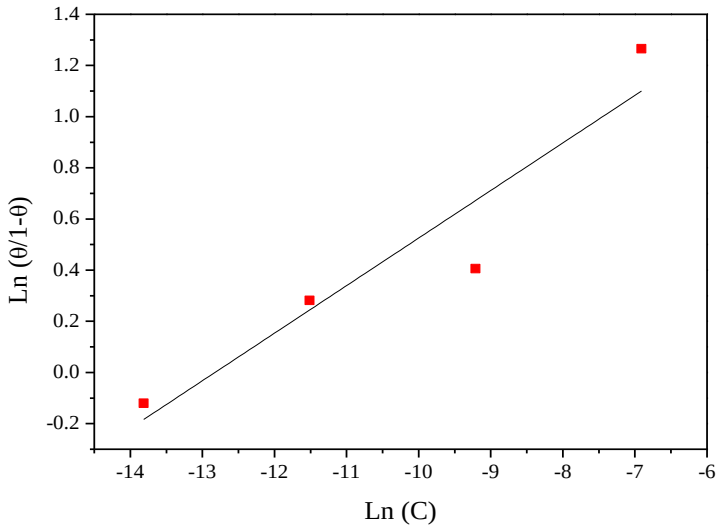

Fig. 4. El-Awady et. al. adsorption isotherm model for carbon steel in 1M HCl containing T1 at 308 K.

Table 3. Adsorption Parameters calculated from the El-Alwady isotherm

Inhibitor	Kads (L/mol)	1/y	ΔG°_{ads} (kJ/mol)
T1	372202.64	5.379	-43.13

The values of 1/y less than one imply multilayer adsorption. In the current work the value of 1/y obtained was more than unity which indicates that each molecule of T1 involved in the adsorption process was attached to more than one active site on the metal surface. The equilibrium constant for the adsorption process was related to the standard free energy of adsorption by the expression

$$\Delta G^{\circ}_{ads} = -RTLn(55.5K_{ads})$$

where R is gas constant and T is absolute temperature of experiment and the constant value of 55.5 is the concentration of water in solution in mol L^{-1}.

Generally, the energy values of -20 kJ mol^{-1}or less negative are associated with an electrostatic interaction between charged molecules and charged metal surface, physisorption; those of -40 kJ mol^{-1} or more negative

involve charge sharing or transfer from the inhibitor molecules to the metal surface to form a coordinate covalent bond, chemisorption [50,51]. The value of ΔG_{ads}° is equal to -43.13 kJ mol^{-1}. The large value of ΔG_{ads}° and its negative sign is usually characteristic of strong interaction and a highly efficient adsorption [52]. The high value of ΔG_{ads}° shows that in the presence of 1M HCl chemisorption of T1 may occur. The possible mechanisms for chemisorption can be attributed to the donation of π-electron in the aromatic rings, the presence of two nitrogen and one sulfur atoms in inhibitor molecule as reactive centers is an electrostatic adsorption of the protonated inhibitor compound in acidic solution to adsorb on the metal surface.
The result indicated that the increase of inhibitor efficiency with concentration may be attributed to the formation of a barrier film, which prevent acid medium to attack the metal surface, because of the adsorption of T1 on the mild metal surface involving interactions between the π-electrons of the heterocyclic structure of benzimidazole and phenyl rings as well as S atom and the vacant d-orbitals of iron surface atoms. We assist clearly to the intramolecular synergistic effect of various adsorption centers of T1 [53].

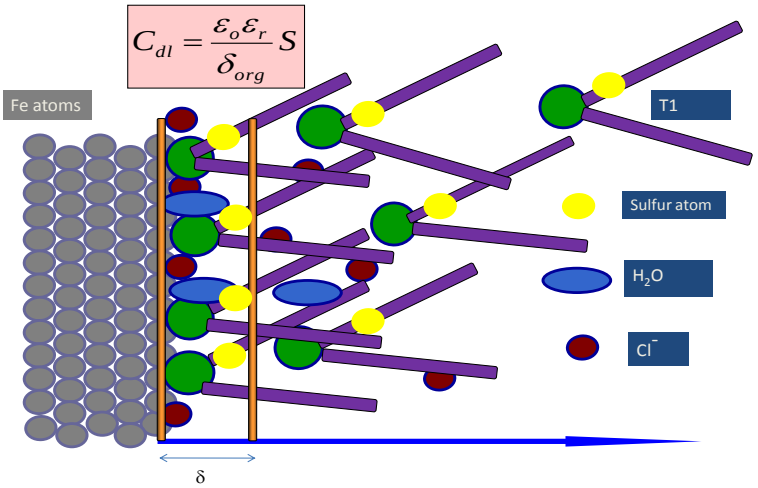

Scheme 1: Actions of different ions/molecules at the metal surface

4. SEM investigation
SEM photographs obtained from carbon steel surface after specimen immersion in 1M HCI solution for 6 h in the absence and presence of 10^{-3} M of T1 are shown in Fig. 5 (a and b).

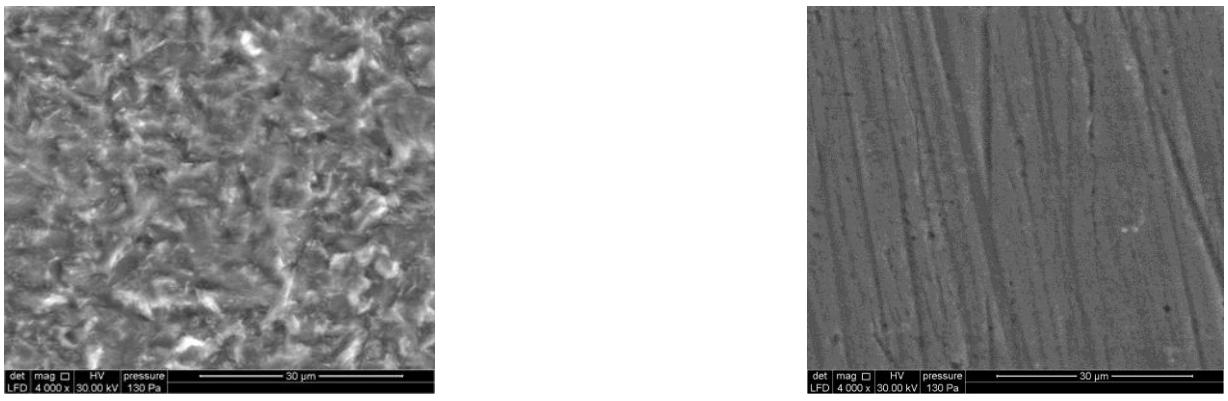

a b

Fig. 5: SEM photographs in the absence "a" and presence "b" of 10^{-3} M of T1

Fig. 5.a shows that the carbon steel surface was strongly damaged in HCl in the absence of T1, Fig. 5.b shows that there is a good protective film adsorbed on the carbon steel surface against corrosion with 10^{-3} M of T1.

5. The potential of zero charge and the inhibition mechanism

All mechanism of corrosion inhibitors are explained by adsorption phenomena. The adsorption mostly depends on the surface charge of the metal, the charge or dipole moment of the inhibitor ions/molecules and the other ions that are specifically adsorbed on to the metal surface [54]. The surface charge of the metal is defined by the position of the open circuit potential with respect to the PZC [55]. The double layer capacitance value depends on the applied DC potential is graphically denoted in Fig. 6. It can be determined according to Antropov et al. [56] by comparing the potential of zero charge (PZC) and the corrosion potential of the metal in the electrolytic medium. As PZC corresponds to a state at which the surface is free from charges, at the stationary (corrosion) potential the metal surface will be positively or negatively charged. Hence, it is necessary to have reliable data about PZC. When carbon steel is immersed in acid solution containing (T1), three kinds of species can be adsorbed on its surface, as described below

(1) If the metal surface is positively charged with respect to PZC, the chloride ions will first get adsorbed on the metal surface. After this first adsorption step, the steel surface will become negatively charged. Hence, the positively charged 2-mercaptobenzimidazole derivative cationic forms will form an electrostatic bond with the Cl^- ions already adsorbed on steel surface. Moreover, the excess positive charge on the electrode surface, Φ ($\Phi = E_{PZC} - E_{corr}$) increases as more inhibitor molecules adsorbed on it [57].

(2) If the metal surface is negatively charged with respect to PZC, the protonated water molecules and 2-mercaptobenzimidazole derivative cationic forms would be directly adsorbed on the metal surface. With increasing negative charge on the metal surface, adsorption of 2-mercaptobenzimidazole derivative molecules increase and its concentration in solution would decrease.

(3) When the metal attains the potential at which the surface charge becomes zero, none of the ions (neither cations nor anions) adsorb on the surface through their ionic center. A few indole molecules may however get physically adsorbed through their planar π orbitals on the metal surface (with vacant π orbitals).

In this study, E_{PZC} = -491 mV, E_{corr} = -460 mV, for carbon steel with addition 10^{-3} M of T1. It can be said that Φ ($\Phi = E_{PZC} - E_{corr}$) potential is positive in this case. From the above result, it follows that anions (Cl^- ions) in aqueous hydrochloric acid solution will be first to get adsorbed on the steel surface. After this first adsorption step, the steel surface will become negatively charged. Hence, the positively charged of 2-mercaptobenzimidazole derivative cationic forms will form an electrostatic bond with the Cl^- ions already adsorbed on steel surface.

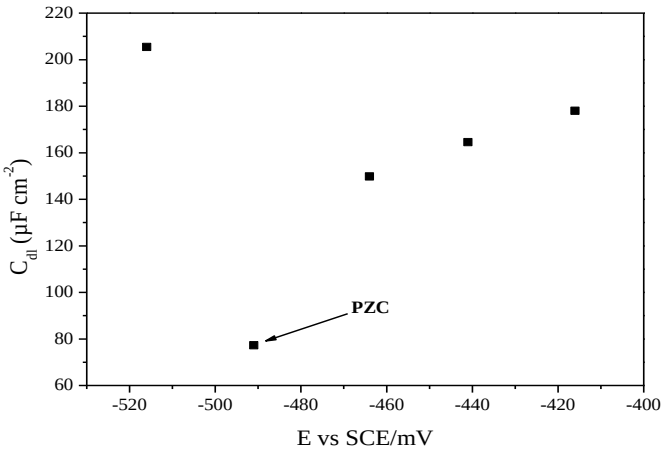

Fig. 6: Plot of C_{dl} vs. applied electrode potential (E, V(SCE)) in 1 M HCl containing 10^{-3} M T1.

6. Molecular Dynamic simulations; adsorption energy calculations.

In the present work, the Molecular Dynamic (MD) simulation Monte Carlo was performed to study the behavior of the system inhibitor/solvent molecules/iron surface [31,32]. The optimization energy curves for T1 inhibitor in the neutral and isolated from using Monte Carlo simulations are presented in Figure 7.

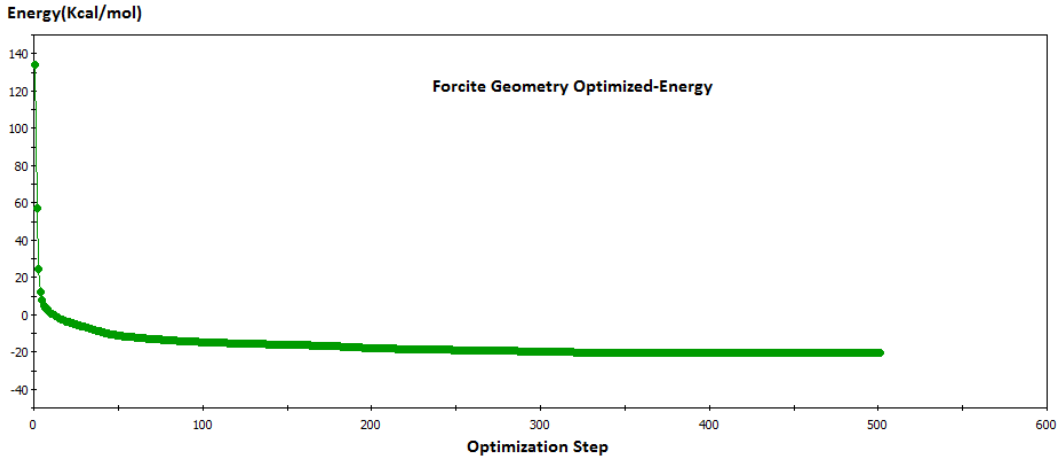

Figure 7 : Optimization energy curves for T1 in the neutral and isolated from using Monte Carlo simulations

The selected T1 inhibitor is placed on the iron surface in the presence of water molecules, optimized and then run quench molecular dynamics. A typical adsorption energy distribution of T1/Fe (111)/30H_2O system consisting of the total energy, average total energy, van der Waals energy, electrostatic energy and intermolecular energy using Monte Carlo simulations are depicted in Figure 8.

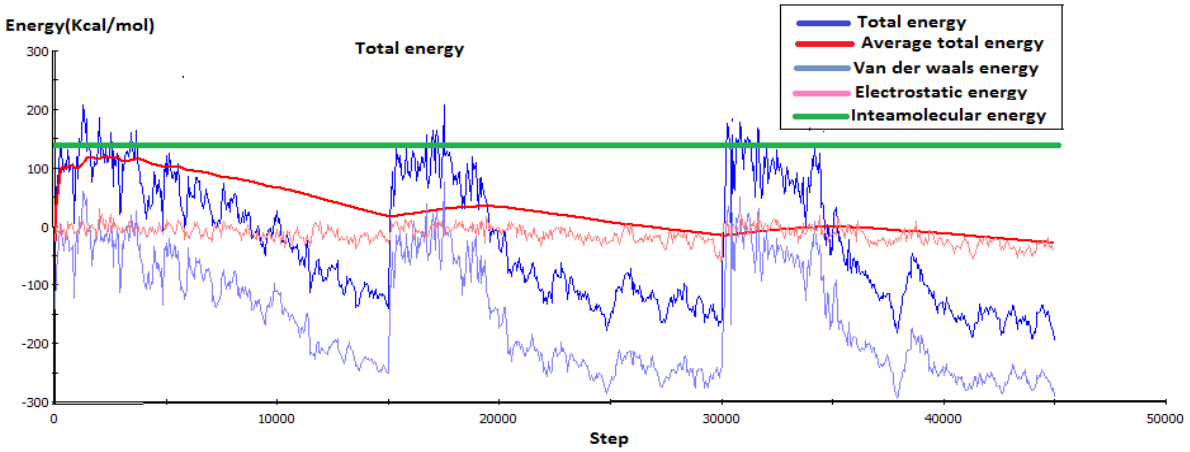

Fig. 8. Typical energy profile for T1/Fe (111)/30H_2O system.

The Metropolis Monte Carlo method in Adsorption Locator calculation provides four step types for a canonical ensemble: conformer, rotation, translation and regrowth [58]. Figure 3 shows the most suitable inhibitor conformation adsorbed on iron surface (111) obtained by adsorption locator module [59]. The most stable low energy adsorption configurations of T1/Fe (111)/30H_2O system using Monte Carlo simulations are presented in both orthogonal and perspective forms in Figure 9.

According to the equilibrium configuration of the T1/Fe (111)/30H_2O system, it is clearly observed that the T1 molecule displaces the water molecules and adsorb onto iron surface (111) in nearly parallel mode (Figure 2). The measured shortest bond distance (Figure 2) between the closest heteroatoms (-N= & -S-) of the T1 inhibitor and iron surface (111) in aqueous phase at equilibrium were as follows: T1–Fe interaction :(Fe–S-=3.294˚A, Fe-N=3.228A° & Fe-N= 3.335A°). All the shortest bond distances were less than3.5˚Aindicating a strong chemical bond formation between the T1 and iron surface (111). However, van der Waals interactions were also involved in the adsorption process of the inhibitor with iron surface (111). The outputs and descriptors calculated by the Monte Carlo simulation, such as the total adsorption, adsorption energy, rigid adsorption and deformation energies are presented in Table 4.

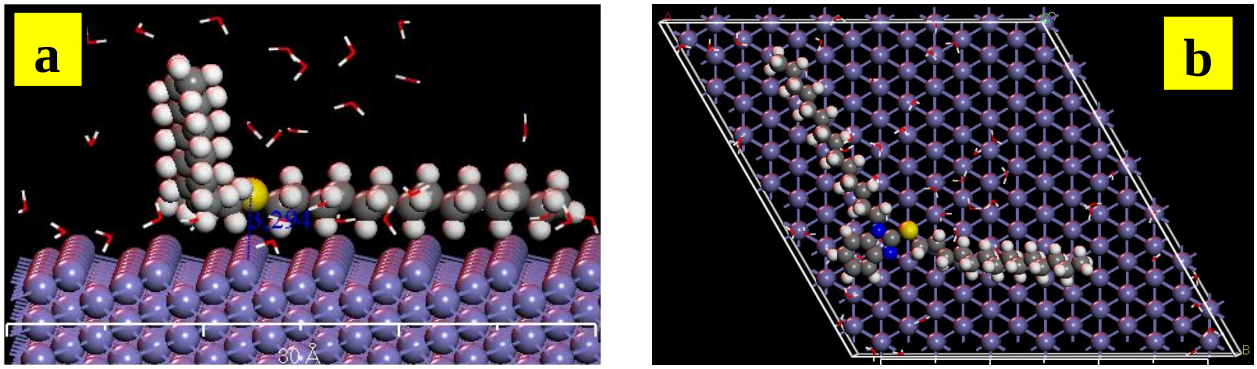

Fig. 9. Perspective (a) & Orthogonal (b) forms of the most stable low energy configuration for T1/Fe (1 11)/30 H_2O system obtained using the Monte Carlo simulations.

Table 4: Outputs and descriptors calculated by the Monte Carlo simulation for the lowest adsorption configurations of T1/ Fe (111)/30H_2O system (all in kcal/moL).

Structures	Total energy	Adsorption energy	Rigid adsorption energy	Deformation energy	T1 : dEad/dNi	H2O : dEad/dNi
Fe (1 1 1) - 1	37,49176330	-234,96288611	-37,55893767	-197,40394844	-199,88826370	-0,95838419
Fe (1 1 1) - 2	42,97272429	-229,48192512	-32,07560847	-197,40631665	-195,16116432	-0,95954433
Fe (1 1 1) - 3	44,04282217	-228,41182723	-30,93570207	-197,47612516	-194,50594998	-0,97875850
Fe (1 1 1) - 4	44,61311212	-227,84153728	-30,28904381	-197,55249347	-191,51471453	-0,96073853
Fe (1 1 1) - 5	44,88136441	-227,57328499	-30,01299908	-197,56028591	-194,03111931	-0,96481478
Fe (1 1 1) - 6	45,16007611	-227,29457330	-29,81132990	-197,48324339	-193,19147335	-0,96744164
Fe (1 1 1) - 7	46,26210732	-226,19254209	-28,64646206	-197,54608003	-190,93146438	-0,96990710
Fe (1 1 1) - 8	46,58260554	-225,87204387	-28,36989865	-197,50214522	-191,75475192	-0,97174620
Fe (1 1 1) - 9	47,12162388	-225,33302552	-27,96862308	-197,36440245	-190,95565975	-0,96312480
Fe (1 1 1) - 10	47,47974643	-224,97490297	-27,37697447	-197,59792850	-190,69355968	-0,95810244

The parameters presented in Table 1 include total energy (E_{Total}) of the T1/ Fe (111)/30H_2O system. The total energy is defined as the sum of the energies of the inhibitor, the rigid adsorption energy (RAE) and the deformation energy (E_{def}). In addition, adsorption energy, in kcal/mol, reports energy released (or required) when the relaxed inhibitor and water molecules (T1/30H_2O) are adsorbed on the iron surface (111). The adsorption energy is defined as the sum of the rigid adsorption energy and the deformation energy for the inhibitor T1. The rigid adsorption energy reports the energy, in kcal/ mol, released (or required) when the unrelaxed inhibitor and water molecules (i.e., before the geometry optimization step) are adsorbed on the iron surface. The deformation energy reports the energy, in kcal/mol, released when the adsorbed molecule are relaxed on the substrate surface. Table 1 shows also that (ΔE_{ads}/dNi), which reports the energy, in kcal/mol, of inhibitor-iron surface configurations where one of the inhibitor has been removed.

It is quite clear from Table 4 that the value of adsorption energies is negative, which denotes that the adsorption could occur spontaneously. The largest negative adsorption energy value indicate the system with the most stable and stronger adsorption [60,61]. In all cases, the adsorption energies of the inhibitor are far higher than that of water molecules. This indicates the possibility of gradual substitution of water molecules from the surface of iron surface resulting in the formation of a stable layer which can protect the iron from aqueous corrosion.

Conclusion

In this work, we have synthesized a new compound derivative of 2-mercaptobenzimidazole susceptive to present interesting surfactant properties. We have shown that the compound present a good inhibition properties for the corrosion of carbon steel in (1M) HCl solution; Polarization curves indicated that the inhibitor behave mainly as mixed-type inhibitor. EIS showed that the charge transfer controls the corrosion process in the uninhibited and inhibited solutions. Different inhibition mechanisms were proposed for T1 molecules, based on their PZC value in studied conditions. The adsorption of T1 followed El-Awady's kinetic-thermodynamic model. Dynamic simulation agrees the displacement of water molecules by the organic inhibitor.

References

1. Hegazy M.A., Novel cationic surfactant based on triazole as a corrosion inhibitor for carbon steel in phosphoric acid produced by dehydrate wet process, *Journal of Molecular Liquids*, 208 (2015) 227-236
2. Wang Q., Ma X., Shi H., (...), Liang, D., Hu, Z., Inhibition performance of benzimidazole derivatives for steel 45(GB) in 1 mol/L HCl solution, *Journal of the Chinese Society of Corrosion and Protection* 35 (2015) 49-54
3. Qiu L.-G., Xie A.-J., Shen Y.-H., A novel triazole-based cationic gemini surfactant: Synthesis and effect on corrosion inhibition of carbon steel in hydrochloric acid, *Mater. Chem. Phys.* 91 (2005) 269-273
4. Maayta A.K., Bitar M.B., Al-Abdalah M.M., *Brit. Corr. J.*, 36 (2001) 133
5. Villamil R.F.V., Corio P.J., Rubin C., Agostinho S.M.L., *J. Electroanal. Chem.*, 472 (1999)112
6. Branzoi V., Golgovici F., Branzoi F., *Mat. Chem. Phys.*, 78 (2002) 122
7. Abd El Aal E.E., Abd El Wanees S., Farouk A., Abd El Haleem S.M., Factors affecting the corrosion behaviour of aluminium in acid solutions. II. Inorganic additives as corrosion inhibitors for Al in HCl solutions, *Corros. Sci.*, 68 (2013) 14
8. Laurence Serreau, Muriel Beauvais, Caroline Heitz, Etienne Barthel, Journal of Colloid and Interface Science, 332 (2009) 382-388.
9. Gaysinski M., Le Forestier J.P., Cambon A., Devoiselle J.M., Maillols H., Chang P., *Journal of Fluorine Chemistry*. 83 (1997) 175-182.
10. Hosseini M., Mertens S.F.L. and Arhadi M. R., Synergism and antagonism in mild steel corrosion inhibition by sodium dodecylbenzenesulphonate and hexamethylenetetramine, *Corros. Sci.*, 45 (2003) 1473
11. Mu G N, Zhao T P, Liu M and Gu T, *Corrosion*, 52 (1996)853
12. Elachouri M., Hajji M.S., Salem M., Kertit S., J. Aride, R. Coudert, E. Essassi, *Corrosion*, 52 (1996) 103
13. Zarrouk A., Zarrok H., Salghi R., Hammouti B., Bentiss F., Touir R., Bouachrine M., Evaluation of N-containing organic compound as corrosion inhibitor for carbon steel in phosphoric acid, *J. Mater. Environ. Sci.* 4 (2) (2013) 177-192
14. Manssouri M., El Ouadi Y., Znini M., Costa J., Bouyanzer A., Desjobert J-M., Majidi L Adsorption proprieties and inhibition of mild steel corrosion in HCl solution by the essential oil from fruit of Moroccan Ammodaucus leucotrichus,., *J. Mater. Environ. Sci.* 6 (3) (2015) 631-646
15. Fouda A.S., Shalabi K., Ezzat R., Evaluation of some thiadiazole derivatives as acid corrosion inhibitors for carbon steel in aqueous solutions, *J. Mater. Environ. Sci.* 6 (4) (2015) 1022-1039
16. Abdel-Azim A.A., Milad R., El-Ghazawy R., Kamal R., Corrosion inhibition efficiency of water soluble ethoxylated trimethylol propane by gravimetric analysis, *Egyptian Journal of Petroleum*, 23 (2014) 15–20
17. Benabdellah M., Tounsi A., Khaled K.F., Hammouti B., Thermodynamic, chemical and electrochemical investigation of 2-mercapto benzimidazole as corrosion inhibitor for mild steel in hydrochloric acid solutions, *Arab. J. Chem*, 4 N°1 (2011) 17-24.
18. Ismaily Alaoui K., Ouazzani F., Kandri rodi Y., Azaroual A.M., Rais Z., Filali Baba M., Taleb M., Chetouani A., Aouniti A., Hammouti B., Effect of some Benzimidazolone compounds on C38 steel corrosion in hydrochloric acid solution, *J. Mater. Environ. Sci.* 7 (1) (2016) 244-258

19. Chakib I., Elmsellem H., Sebbar N. K., Lahmidi S., Nadeem A., Essassi E. M., Ouzidan Y., Abdel-Rahman I., Bentiss F., Hammouti B., Electrochemical, gravimetric and theoretical evaluation of (4Z)-2,5-dimethyl-4-(4-methylpyrimido[1,2- a]benzimidazol-2(1H)-ylidene)-2,4-dihydro-3H-pyrazol-3-one (P1) as a corrosion inhibitor for mild steel in 1 M HCl solution, *J. Mater. Environ. Sci.* 7 (6) (2016) 1866-1881
20. Morales-Gil P., Walczak M.S., Cottis R.A., Romero J.M., Lindsay R., Corrosion inhibitor binding in an acidic medium: Interaction of 2-mercaptobenizmidazole with carbon-steel in hydrochloric acid *Corros. Sci.* 85 (2014) 109-114
21. Forsal I., Ebn Touhami M., Mernari B., El Hajri J., Filali Baba M., Use of experimental designs to evaluate the influence of 2-mercaptobenzimidazole on the corrosion of mild steel in HCl (1 M) environment in the presence of alcohol ethoxylate, *Portugaliae Electrochimica Acta* 28 (2010 203-212
22. Leen C. Davidse, *Ann. Rev. Phytopathol*. 24 (1986) 43-65.
23. Yogita Bansal, Om Silakari, *Bioorg. Med. Chem.* 20 (2012) 6208–6236.
24. Ingle R.G, Magar D.D, *International Journal of Drug Research and Technology.* 1 (2011) 26-32.
25. Namrata Singh, Annamalai Pandurangan, Kavita Rana, Preeti Anand, Arshad Ahmad, Amit Kumar Tiwari, *International Current Pharmaceutical Journal*. 1(5) (2012) 119-127.
26. Ramanpreet Walia, Md. Hedaitullah, Syeda Farha Naaz, Khalid Iqbal and HS. Lamba, *International Journal of Research in Pharmacy and Chemistry*. 1(3) (2011) 565-574.
27. Singh Gurvinder, Kaur Maninderjit, Chander Mohan, *International Research Journal of Pharmacy*, 4(1) (2013) 82-87.
28. Sreenivasulu Enumula, Anees Pangal, Muiz Gazge, Javed A. Shaikh and Khursheed Ahmed, *Research Journal of Chemical Sciences*, 4(4) (2014) 78-88.
29. Materials Studio version 7.0, Accelrys Inc. USA, 2013.
30. Belghiti M.E., Karzazi Y., Dafali A., Obot I.B., Ebenso E.E., Emrane K.M., Bahadur I., Hammouti B., Bentiss F., *J. Mol. Liq.* 216 (2016) 874–886.
31. ElBelghiti M., Karzazi Y., Dafali A., Hammouti B., Bentiss F., Obot I.B., Bahadur I., Ebenso E.E.. *J. Mol. Liq.* 218 (2016) 281–293.
32. H. Sun, P. Ren, J.R. Fried, The COMPASS force field: parameterization and validation for phosphazenes, *Comput. Theory. Polyp. Sci.* 8 (1998) 229-246.
33. Guo L., Zhu S., Zhang S., He Q., Li W., Theoretical studies of three triazole derivatives as corrosion inhibitors for mild steel in acidic medium, *Corros. Sci.* 87 (2014) 366.
34. Jutner K., Electrochemical impedance spectroscopy (EIS) of corrosion processes on inhomogeneous surfaces, *Electrochim. Acta* 35 (10) (1990) 1501
35. Manssouri M., El Ouadi Y., Znini M., Costa J., Bouyanzer A., Desjobert J-M., Majidi L., Adsorption proprieties and inhibition of mild steel corrosion in HCl solution by the essential oil from fruit of Moroccan Ammodaucus leucotrichus, *J. Mater. Environ. Sci.* 6 (3) (2015) 631-646
36. Fouda A.S., Mostafa H.A., El-Taib F., Elewady G.Y., Synergistic influence of iodide ions on the inhibition of corrosion of C-steel in sulphuric acid by some aliphatic amines, *Corros. Sci.* 47 (2005) 1988–2004
37. Bockris J.O'M, Swinkels D.A.J., *J. Electrochem. Soc.*, 111 (1964) 736
38. Emregu K. C., Hayval M., Studies on the effect of a newly synthesized Schiff base compound from phenazone and vanillin on the corrosion of steel in 2 M HCl, *Corros. Sci.*, 48 (2006) 797-812
39. Khadraoui A., Khelifa A., Hamitouche H., Mehdaoui R., Inhibitive effect by extract of Mentha rotundifolia leaves on the corrosion of steel in 1 M HCl solution, *Res. Chem. Intermed.* 40 (2014) 961–972
40. El-Hajjaji F., Greche H., Taleb M., Chetouani A.,, Aouniti A., Hammouti B., Application of essential oil of thyme vulgaris as green corrosion inhibitor for mild steel in1M HCl,., *J. Mater. Environ. Sci.* 7 (2016) 566-578.
41. Cao C., On electrochemical techniques for interface inhibitor, *Corros. Sci.*, 38 (1996) 2073-2082
42. Villamil R.F.V., Corio P., Agostinho S.M.L., Rubin J.C., *J. Electroanal. Chem*. 472 (1999) 112.
43. Trabanelli G., in: Mansfeld F (Ed.), Corrosion mechanism, Mercel Dekker, New York, 2006
44. McCafferty E., in: Leidheiser Jr. H (Ed.), Corrosion control by coating, Science Press, Princeton, 1979

45. Khamis E., The effect of temperature on the acidic dissolution of steel in the presence of inhibitors, *Corrosion* 46 (1990) 476.
46. Abd El-Rehim S.S., Magdy A., Ibrahim A.M., Khaled K.F., *J. Appl. Electrochem*. 29 (1999) 593.
47. Moretti G., Quartarone G., Tassan A., Zingales A., *Mater. Corros*. 45 (1994) 641.
48. Ibot I.B., Obi-Egbedi N.O., Umoren S.A., *Int. J. Electrochem. Sci*. 4 (2009) 863.
49. Singh A.K., Quraishi M.A., *Corros. Sci. 53* (2011) 1288.
50. Donahue F.M., *J. Electrochem. Soc*. 112 (1965) 886.
51. Khamis E., Bellucci F., Latanision R.M., El-Ashry E.S.H., *Corrosion*, 47 (1991) 677-686.
52. Abdallah M., Rhodanine azosulpha drugs as corrosion inhibitors for corrosion of 304 stainless steel in hydrochloric acid solution, *Corros. Sci*. 44 (2002) 717.
53. Krim O., Elidrissi A., Hammouti B., Ouslim A., Benkaddour M., Synthesis, characterization and comparative study of new pyridine derivatives as inhibitors of corrosion of mild steel in hydrochloric acid medium, *Chem. Eng. Comm.* 196 (2009) 1536-1546.
54. Ma H., Chen S., Yin B., Zhao S., Liu X., Impedance spectroscopic study of corrosion inhibition of copper by surfactants in the acidic solutions, *Corros. Sci*. 45 (2003) 867.
55. Solmaz R., Mert M.E., Kardas G., Yazici B., Erbil M., *Acta Phys. Chem. Sinica* 24(7) (2008) 1185.
56. Antropov L.I., Makushin E.M., Panasenko V.F., Technika, Kiev, 1981. p.182.
57. Hackerman N., Makrids A.C., *J. Phys. Chem*. 59 (1955) 707.
58. Guedes Soares C., Garbatov Y., Zayed A., Wang G., Corrosion wastage model for ship crude oil tanks *Corros. Sci.*, 50 (2008) 3095-3106.
59. Tan Y., Understanding the effects of electrode inhomogeneity and electrochemical heterogeneity on pitting corrosion initiation on bare electrode surfaces, *Corros. Sci*., 53 (2011) 1845-1864 / Gudze M.T., Melchers R.E., Operational based corrosion analysis in naval ships, *Corros. Sci.*, 50 (2008) 3296-3307.
60. Kumar A. M., Babu R. S., Obot I. B., Zuhair, Gasem M., *RSC Adv*. 5 (2015) 19264-19272.
61. Obot I.B., Umoren S.A., Gasem Z.M., Suleiman R., El Ali B., Theoretical prediction and electrochemical evaluation of vinylimidazole and allylimidazole as possible green corrosion inhibitors for carbon steel in 1 M HCl, *J. Ind. Eng. Chem.* 21 (2015) 1328–1339.